

Article

Composite Collectors for the Flotation of Refractory Alkaline Rock-Type Rare-Earth Ores

Chunfeng Li ^{1,2}, Zhichao Liu ^{2,*}, Zhenjiang Liu ¹, Jiajun Liu ¹, Guang Li ², Yuhui Tian ² and Mingliang Zhou ³

¹ School of Earth Sciences and Resources, China University of Geosciences, Beijing 100083, China; licf_cugb@163.com (C.L.); lzj@cugb.edu.cn (Z.L.); liujiajun@cugb.edu.cn (J.L.)

² Beijing Research Institute of Chemical Engineering and Metallurgy, CNNC, Beijing 101149, China; hmlghappy@163.com (G.L.); tyh719368434@126.com (Y.T.)

³ School of Resources and Civil Engineering, Northeastern University, Shenyang 110819, China; 2010406@stu.neu.edu.cn

* Correspondence: zcliu1006@bricem.com.cn; Tel.: +86-010-5167-4319

Abstract: Alkaline rock-type rare-earth (RE) ores have significant utilisation value. However, the exploitation of such resources faces great challenges owing to the complex mineral and element assemblages. Composite collectors exhibit excellent performances, which may provide solutions to the flotation problem of alkaline rock-type RE ores. Therefore, 16 collectors typically used in RE ores flotation were selected. Flotation tests were performed to identify collectors with high selectivity and collection ability for RE minerals, then nine composite collectors were prepared by combining the satisfactory collectors. The flotation performances of single and composite collectors for RE minerals were examined, and the composite collector FA301 with different carbon chain lengths was identified as the best one. When FA301 was applied in optimal conditions of slurry temperature, grinding size, collector and inhibitor dosage, RE concentrate yield of 6.29%, REO grade of 32.013%, and recovery of 59.02% were achieved. According to the results of the zeta potential, FTIR, and XPS test, the functional groups (dominated by carboxyl groups) in FA301 chemically adsorbed onto the main active sites (La, Ce, Y, etc.) on the surface of RE minerals. The findings can provide scientific basis for the development of efficient collectors to facilitate the exploitation of RE resources.

Keywords: alkaline rock-type; RE ore; composite collector; flotation process; mechanism of flotation



Citation: Li, C.; Liu, Z.; Liu, Z.; Liu, J.; Li, G.; Tian, Y.; Zhou, M. Composite Collectors for the Flotation of Refractory Alkaline Rock-Type Rare-Earth Ores. *Minerals* **2023**, *13*, 1025. <https://doi.org/10.3390/min13081025>

Academic Editors: Richmond K. Asamoah, Ahmet Deniz Baş, George Blankson Abaka-Wood, Kali Sanjay and Jonas Addai-Mensah

Received: 26 June 2023
Revised: 20 July 2023
Accepted: 27 July 2023
Published: 31 July 2023



Copyright: © 2023 by the authors. Licensee MDPI, Basel, Switzerland. This article is an open access article distributed under the terms and conditions of the Creative Commons Attribution (CC BY) license (<https://creativecommons.org/licenses/by/4.0/>).

1. Introduction

Rare-earth (RE) elements (REEs) refer to 17 elements that include 15 lanthanides (atomic numbers 57–71) and yttrium (Y) and scandium (Sc) of Group IIIB in the periodic table. REEs play an irreplaceable role in traditional fields such as medical treatment, agriculture, metallurgy, and ceramics, and high-tech fields such as aerospace and military [1,2]. Therefore, REEs represent a key strategic resource for economic development and social progress [3].

Dostal [4] divided RE deposits into four types according to their production environment: carbonate-hosted deposits, alkaline rocks-host deposits, ion-adsorption deposits, and placer deposits. Alkaline rock-type RE ores are the second most valuable RE resources, following carbonate RE ores. Heavy REEs are enriched in the ores, characterised by strategic metals such as uranium (U), niobium (Nb), zirconium (Zr), beryllium (Be), thorium (Th), and hafnium (Hf) [4–7], which have high economic value. Owing to the variety of metals and their low grades [6], RE minerals in alkaline rock-type ores typically need to be enriched through beneficiation to decrease development costs and promote the comprehensive recovery and utilisation of the different metals.

Flotation is the most commonly used technology for the mineral separation of carbonate RE ores [8–10], which is the most valuable RE resource worldwide. Although more

than 30 alkaline rock RE deposits exist in the world [11], only the Kola Peninsula deposit in Russia with a single type of RE mineral is currently being exploited [4]. Unlike the mature flotation technologies for carbonate RE ores, the flotation of alkaline rock RE ores involves many challenges. The main mineral composition of alkaline rock RE deposits is more complex than that of carbonate RE deposits [6]. Moreover, in addition to common carbonate and phosphate RE minerals, alkaline rock RE ores contain different silicate and oxide RE minerals [4,12,13].

A lot of research achievements have been accumulated in terms of collectors and flotation mechanism for the major and industrially utilised rare-earth minerals in carbonate rare-earth ores such as bastnaesite, monazite, xenotime, etc. [10]. The roles of fatty acids and hydroxamic acids as collectors in the flotation of RE minerals have been extensively studied. Carboxylic acids, represented by fatty acids, have been preferentially used as reagents for RE mineral flotation [8], such as sodium oleate (NaOl) [14,15], oxidised paraffin soap [16], and tall oil [17]. However, these acids exhibit low selectivity. To address this problem, hydroxamic acid has been used in the flotation of RE minerals such as bastnaesite, monazite, and xenotime. For example, salicylhydroxamic acid [18], benzohydroxamic acid [19,20], C5-9 alkyl hydroxamic acid [21], and H205 applied to the flotation of Bayan Obo RE ore [22]. Hydroxamic acid collectors form highly stable chelates with Fe^{3+} and Al^{3+} , followed by REEs [23,24]. In other words, when a flotation system involves many iron (Fe)-containing minerals, the selectivity of hydroxamic acid collectors is low. In addition, organic phosphoric acid [25], sulfonates [26,27], and ionic liquid [28] collectors exhibit a certain collection effect on RE minerals. Notably, the existing studies on collectors have focused on carbonate and phosphate RE minerals, and only a few researchers have examined the flotation of silicate (gadolinite and allanite) and oxide RE minerals (fergusonite) with simple mineral compositions [9,29,30]. Reports on the flotation of complex RE mineral systems containing carbonate, phosphate, silicate, and oxide are rare. In particular, research on the flotation of alkaline rock-type RE ores with Fe-bearing minerals (arfvedsonite, aegirine, and columbite) and high field strength elements (U, Zr, Nb, etc.) minerals is limited.

As mentioned previously, hydroxamic acid collectors are associated with low collection capacity and high costs [31–33]. Moreover, fatty acids have low dispersity and need to be heated in the flotation process [8]. Researchers have focused on composite collectors to address these problems [34–36]. Xu et al. [37] developed a composite collector using octylhydroxamic acid and NaOl that enhanced the flotation recovery of bastnaesite with limited collector consumption. Bao et al. [38] used a terpolymer collector composed of oleic acid, methyl oleate, and diesel oil to achieve enhanced selectivity, collection, and dispersion ability. Luo et al. [39] used benzohydroxamic acid and dodecylamine as a compound collector and noted that dodecylamine enhanced the selectivity and collection ability of benzohydroxamic acid through co-adsorption. Qiao et al. [40] improved the solubility and collection ability of dodecylamine by combining it with 2-octanol–kerosene. Despite the promising collaborative collection effect of composite collectors, their application to RE mineral flotation is limited. The effects of composite collectors on actual ores, especially alkaline rock-type RE ores, must be further explored.

The Baerzhe deposit in Inner Mongolia, China, is a typical super-large alkaline rock-type RE deposit characterised by U, Zr, Nb, Be, and other metals. The characteristics and element and mineral compositions of Baerzhe ore are similar to those of many alkaline rock RE minerals found in China and other countries [6,41], and thus, it is an ideal research object for examining the flotation of alkaline rock-type RE ores. The grades of the REEs and other useful elements in the ore are low, and thus, the ore's economic utilisation is possible only through beneficiation. At present, RE beneficiation is performed as follows: the raw ore is pre-enriched by high-intensity magnetic separation (HIMS), and RE concentrates are then obtained by the flotation of high-intensity magnetic concentrates [27,42]. Notably, Fe-containing minerals with physical properties similar to those of RE minerals [43], such as arfvedsonite and columbite, cannot be easily separated by gravity magnetic separation and tend to enter the RE flotation system, resulting in complex mineral assemblage and

deterioration of the flotation environment. Moreover, the pulp in the existing RE flotation must be heated to above 50 °C and the selectivity of the collector is low, which limits the economic benefits of flotation processes.

The objective of this study was to realise the RE mineral flotation of the Baerzhe mine. The existing RE mineral collectors were systematically compared in flotation tests, effective collectors were screened, and different composite collectors were prepared for the flotation of RE concentrates. The mode of adsorption of the collectors onto the surface of the RE minerals was identified by zeta potential testing. The key groups in the collectors were categorised by Fourier transform infrared spectroscopy (FTIR), and the adsorption sites of the collectors on the surface of RE minerals were clarified by X-ray photoelectron spectroscopy (XPS). The findings can provide reference for the development of efficient collectors that can facilitate the utilisation of RE resources in the Baerzhe deposit and enhance the understanding of the sorting mechanism of alkaline rock-type RE ores.

2. Materials and Methods

2.1. Samples and Reagents

2.1.1. Samples

Flotation samples: Baerzhe Run-of-mine (ROM) ores with [REO] grade of 0.995% were collected, sampled, ground to a fineness of 50% < 74 µm, and treated by HIMS at a magnetic induction intensity of 1.4 T [44] to prepare HIMS concentrates as the head samples for flotation.

Mineral samples: the pure mineral samples of hingganite, monazite, and bastnaesite used in the examination of the flotation mechanism were obtained from the Baerzhe deposit. ROM ores were crushed, ground in a ball mill (XMCQ-φ180 × 200) with zirconium ball as grinding medium at 50% of the grinding mass concentration, and separated by gravitational and HIMS to obtain the pre-concentration concentrate. Hingganite, monazite, and bastnaesite were separated from the pre-concentration concentrate through manual selection under a microscope based on differences in the colour and gloss levels. The three mineral samples were washed three times with deionised water and dried at 60 °C.

2.1.2. Reagents

The flotation collectors used in this study included: carboxylic acids, hydroxamic acid, sulfonate, and phosphoric acids. Sodium silicate (WG), magnesium fluosilicate, deionised water and other reagents were also used in flotation experiments. The specific descriptions of the reagents used in this study are listed in Table S1 (see the Supplementary Materials).

2.2. Experiments

2.2.1. Flotation Test for Collector Screening

The effects of single and composite collectors on the flotation of RE ore were investigated. All flotation tests were conducted in an XFD 1.5 L (Jilin Prospecting Machinery Factory, Changchun, China) self-aspirated hanging tank flotation machine at a stirring speed of 1920 r/min. The pulp was adjusted to the desired temperature by using an electric heating rod and a thermostat.

The flotation was performed with one stage of roughing, one stage of scavenging, and multiple stages of cleaning. The HIMS concentrate was ground to a particle size of 90% < 38 µm as feed; the pulp temperature and pH were 40 °C and 8.6 ± 0.2, respectively; the flotation mass concentration was 30%; the dosages of regulator (Na₂CO₃), inhibitor (WG), and activator (MgSiF₆) in roughing were 1 kg/t, 1800 g/t, and 300 g/t, respectively. The dosages of each collector in roughing and scavenging were 400 g/t and 200 g/t, respectively. The rough concentrate was further cleaned several times without any reagents. Figure 1 shows the tests process and stirring time for each part. The pulp pH was adjusted using NaOH and H₂SO₄ solutions in this study.

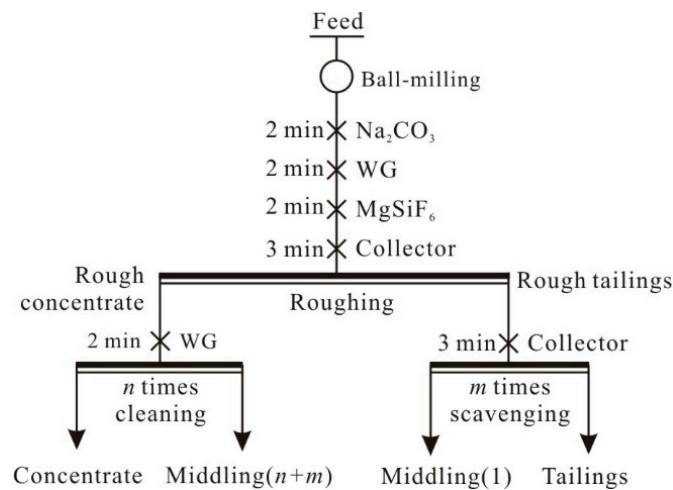


Figure 1. Test process for rare-earth flotation conditions.

After the test, the foam and tank products were collected, filtered, dried, and weighed. Subsequently, the yield was calculated, representative samples were extracted, and REO grade was determined. The cumulative grade and recovery of REO in different products were calculated using Equations (2) and (3), and the flotation performance of each collector was analysed.

$$\beta_{raw} = \gamma_C \beta_C + \gamma_T \beta_T + \sum_{i=1}^{n+m} \gamma_i \beta_i \quad (1)$$

$$\beta_{cum} = (\gamma_C \beta_C + \sum_{i=x}^{n+m} \gamma_i \beta_i) / (\gamma_C + \sum_{i=x}^{n+m} \gamma_i) \quad (2)$$

$$\varepsilon_{cum} = (\gamma_C \beta_C + \sum_{i=x}^{n+m} \gamma_i \beta_i) / \beta_{raw} \quad (3)$$

where β and ε are the grade and recovery of REO; γ is the yield; γ_T and β_T are the yield and REO grade of tailings; γ_i and β_i are the yield and REO grade of middling(i); subscripts C , T , raw , and i represent the concentrate, tailings, raw ore, and middling(i), respectively; cum represents the cumulative indicator (grade or recovery) of concentrate and middling(x)~($n + m$); and n and m represent the number of cleaning and scavenging steps, respectively.

2.2.2. Flotation Condition Test

Slurry temperature and collector dosage conditions were determined through flotation tests involving one roughing stage and five scavenging stages, which were conducted at temperatures of 35, 40, 45, and 50 °C. The dosages of Na_2CO_3 , WG, and MgSiF_6 in roughing were 1 kg/t, 1.8 kg/t, and 300 g/t, respectively. A certain amount of the collector (100 g/t) was added before roughing and each scavenging stage, with the cumulative dosage of the collector being 600 g/t. The feed fineness was $90\% < 38 \mu\text{m}$, flotation concentration was 30%, and pulp pH was 8.6 ± 0.2 . Full factor flotation tests were conducted to determine the optimal slurry temperature and collector dosage combination.

To determine grinding fineness, inhibitor and activator dosage conditions, single factor variable flotation experiments were performed involving one roughing stage, several scavenging stages, and cleaning stages. The specific test conditions and processes are shown in Table S2.

2.2.3. RE Minerals Treatment

The three RE minerals—hingganite, monazite, and bastnaesite—were ground to $74 \mu\text{m}$ in an agate mortar. Half the amounts of the three RE mineral samples were mixed with the collector in a beaker and stirred for 12 h under the optimal conditions determined in the flotation tests, after which the pulp was removed. The flotation slurry was centrifuged

and precipitated for 3 min at a rotating speed of 7500 r/min. The collector included in the sediment was removed by washing with deionised water. The sample was dried at a low temperature of 60 °C for 4 h, ground evenly with an agate mortar, and stored in a desiccator for the characterisations.

2.3. Characterisations

2.3.1. Mineralogical Analysis

Inductively-coupled plasma mass spectrometer (ICP-MS) and chemical analysis were used for chemical composition analysis. An advanced mineral identification and characterisation system (AMICS) was employed to characterise the HIMS concentrates which consists of scanning electron microscopy (SEM, ZEISS Siga 300) with X-ray energy dispersive spectrometer (EDS, Bruker XFlash 6/30) and the software package developed by Bruker (Karlsruhe, Germany). The modal mineralogy of the samples was analysed by the XMOD-std method. The distribution of elements in minerals was analysed using Sankey diagram by Origin software. The intergrowth relationship and proportion of RE minerals and gangue minerals was analysed using Chord diagram by Origin software. The RE mineral samples were analysed by SEM.

2.3.2. Zeta Potential Measurements

The zeta potentials different pH values were measured using a zeta potential analyser (90Plus PALS, Bruker, Billerica, MA, USA) equipped with a rectangular electrophoresis cell at 25 °C. Mineral suspensions containing 0.02 g of RE minerals (<10 µm) and 40 mL KCl solution (1 mM) were prepared in a beaker at a given pH and reagent concentration. The pH of the solution was adjusted with drops of H₂SO₄ or NaOH solutions to vary between 2 and 12 pH units. After allowing the suspension to settle for 5 min, 10 mL of the supernatant liquor was transferred to a measurement cell, the zeta potential was measured three times, and the averaged value was used as the final result.

2.3.3. FTIR Spectra

The FTIR spectra of the three RE minerals before and after collector adsorption were recorded in the range of 400 to 4000 cm⁻¹ at room temperature (25 °C) using Tensor II (Bruker Co., Billerica, MA, USA). Specifically, 0.5 g of hingganite, monazite, or bastnaesite (<38 µm) was individually suspended in 200 mL of the collector solutions for 24 h at 40 °C and pH 8.6 ± 0.2 in a beaker. Next, the pulps were centrifuged and gently washed three times with deionised water to remove the weakly bound physisorbed species. The samples were dried in a vacuum oven for 24 h at 45 °C before obtaining the FTIR scans. Each RE mineral (50 mg) was mixed with 500 mg of KBr powder in an agate mortar. The mixture was ground to decrease the particle size and promote complete mixing. Subsequently, the powdered mixture was pressed into a semi-transparent thin plate for FTIR analysis.

2.3.4. XPS Test

An X-ray photoelectron spectrometer (Escalab 250xi) was used to examine the elemental composition and valence state of the mineral surface before and after flotation. A single monochromatic Al-Kα X-ray source (1486.6 eV) was used, and the test area, pressure, and energy were 500 µm, <10⁻⁷ Pa, and 20 eV, respectively. The full spectrum step was 1 eV, and the single element narrow scan step was 0.1 eV. Binding energy values were calibrated using characteristic carbon (C1s = 284.8 eV) during data processing of XPS spectra. The data were analysed using Thermo Avantage v5.9922 software, with the standard peak values of the binding energy of all elements extracted from the work of Naumkin et al. [45].

3. Results and Discussion

3.1. Modal Mineralogy

The chemical and mineral compositions of HIMS concentrates are displayed in Tables 1 and S3. The valuable elements REO, ZrO₂, Nb₂O₅ and U in the sample (HIMS con-

centrate) have contents of 3.33%, 6.77%, 1.05% and 0.052%, respectively. The distribution of REEs, U, Zr and Nb in different minerals is shown in Figure 2. REEs were mainly in the form of silicate (hingganite and allanite), phosphate (monazite), carbonate (bastnaesite), and a few oxide (aeschnite and pyrochlore) minerals.

Table 1. Chemical composition of the as-prepared HIMS concentrates (wt %).

REO	ZrO ₂	Nb ₂ O ₅	U	HfO ₂	ThO ₂	Ta ₂ O ₅	TiO ₂	SiO ₂	Fe ₂ O ₃	Al ₂ O ₃	Na ₂ O	CaO	K ₂ O	MgO	MnO
3.33	6.77	1.05	0.052	0.167	0.236	0.099	2.51	55.74	14.65	7.52	4.53	0.264	1.78	0.126	0.504

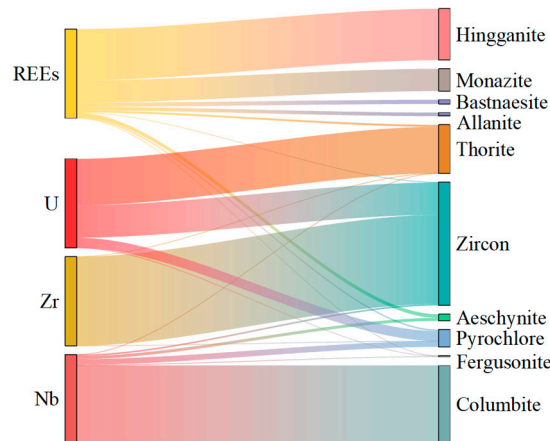


Figure 2. Sankey diagram of REEs, U, Zr, and Nb distribution in different minerals.

The SEM images of RE minerals in Figure 3 show the appearance of hingganite, monazite, bastnaesite, aeschnite, and pyrochlore in HIMS concentrate. The intergrowth relationship and proportion of RE mineral and gangue minerals are shown in Figure 4, in which the area of RE mineral represents the relative content and the arrow width represents the intergrowth proportion. RE minerals are closely related to gangue minerals such as quartz, kaolinite, orthoclase, and so on. Figure 5 shows the SEM images of the three main RE minerals used for flotation mechanism research: hingganite (silicate), monazite (phosphate), and bastnaesite (carbonate). The energy spectrum data of the three RE minerals is shown in Figure S1 (see the Supplementary Materials).

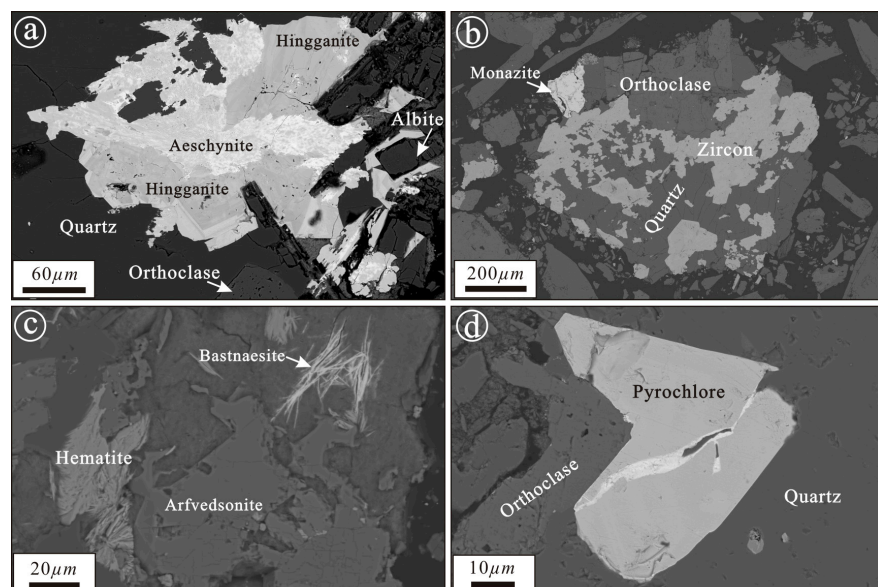


Figure 3. SEM images of RE minerals, hingganite, monazite, bastnaesite, aeschnite, and pyrochlore.

(a) hingganite associated with quartz surrounds albite and interspersed with aeschynite; (b) monazite closely associated with orthoclase and quartz containing zircon; (c) bastnaesite and hematite distributing near amphibole; (d) pyrochlore surrounded by quartz and orthoclase.

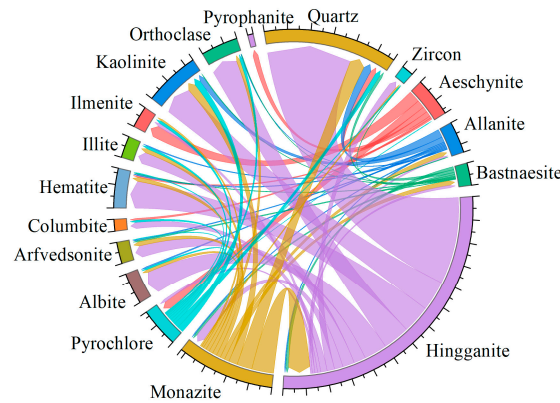


Figure 4. Chord diagram of the intergrowth relationship between RE mineral and gangue minerals.

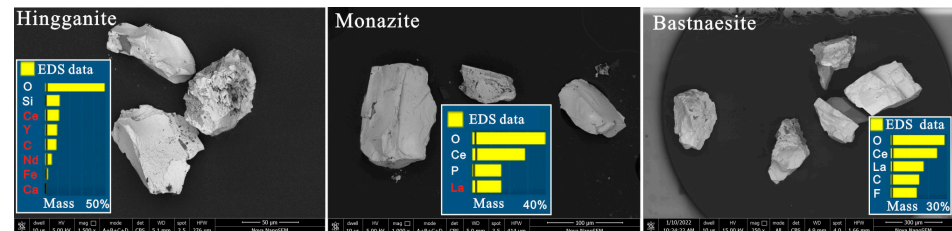


Figure 5. SEM images and energy spectra of RE minerals: hingganite, monazite, and bastnaesite.

3.2. Collector Selection

The collector considerably influences the flotation performance. To identify the optimal collectors for RE minerals of Baerzhe ore, the influence of different collectors on the flotation effect was systematically investigated.

3.2.1. Flotation Indices of Single Collectors

Figure 6 shows the relationships between the cumulative REO grade and recovery of flotation RE concentrates for different single collectors.

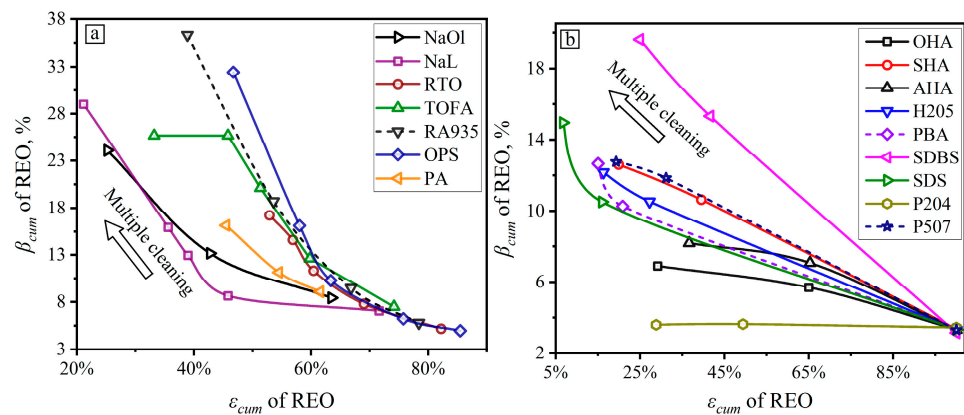


Figure 6. Relationship between the cumulative REO grade and recovery of concentrates for different collectors: (a) fatty acid collectors; (b) hydroxamic acid, organic phosphoric acid, and sulfonate collectors.

As shown in Figure 6a, sodium oleate (NaOl), sodium linoleate (NaL), and phthalic acid (PA) exhibited the lowest selectivity and collection ability among carboxylic acid (salts)

collectors, and the other four collectors exhibited similar collection abilities when the REO recovery was 60%–70%. Oxidised paraffin soap (OPS) and RA935 exhibited the highest selectivities, followed by tall oil fatty acid (TOFA) and refined tall oil (RTO). Notably, NaOl and NaL are C18 fatty acids with a single carbon chain length, whereas the other four collectors are mixed carboxylic acid (salts) reagents with carbon chain lengths of C8–C20, attributable to the wide variety of RE minerals in the Baerzhe ore.

As shown in Figure 6b, the selectivities and collection abilities of the five hydroxamic acid collectors (OHA, SHA, AHA, H205, PBA) were not as high as those of the carboxylic acid collectors. The REO grade in the flotation concentrate was lower than 14%, and the recovery was only approximately 20%. Therefore, hydroxamic acid collectors are not suitable for the flotation of RE concentrates of such ores. The two organic phosphate collectors (P204 and P507) exhibited low selectivities and collection abilities. In contrast, P507 exhibited high selectivity and collection ability, similar to those of salicylic hydroxamic acid. Among the sulfonate collectors, sodium dodecyl benzene sulfonate (SDBS) exhibited high selectivity and collection ability. When the REO grades of the flotation concentrate were 15.3% and 20%, the recoveries were approximately 41.6% and 25%, respectively. Compared with the carboxylic acid (salts) collectors, sulfonate collectors are not suitable for RE concentrate flotation of the minerals in Baerzhe ore.

3.2.2. Flotation Indices of Composite Collectors

As discussed, mixed carboxylic acids (salts) with different carbon chain lengths can better collect RE minerals than the acids with a single carbon chain length. To enhance the collector performance, the collectors with satisfactory flotation performances were combined, as indicated in Table 2.

Table 2. Composite collectors for RE mineral flotation.

Series	Composite Collector	Mass Ratio
L	L1	RA935, H205, PBA, EA, and NaOH: 30:3:3:5:5
	L2	RA935, PA, PBA, EA, and NaOH: 30:3:3:5:5
	L3	RA935, PBA, AHA, EA, and NaOH: 20:3:13:5:5
	L4	RA935, H205, EA, and NaOH: 30:3:5:5
FHP		RA935, PBA, AHA, P204, P507, EA, and NaOH: 15:4:7:5:5:5
NQL	NQL1	RA935, SDBS, EA, and NaOH: 30:3:5:5
	NQL2	RA935, SDS, EA, and NaOH: 30:3:5:5
FA	FA201	RA935, OPS, Tween 80, and NaOH: 3:3:1:1
	FA301	RA935, OPS, RTO, Tween 80, and NaOH: 2:2:2:1:1

L-series collectors consist of carboxylic acids, hydroxamic acids, and emulsifiers. FHP collector consists of carboxylic acids, hydroxamic acids, organic phosphoric acids, and emulsifiers. NQL-series collectors consist of carboxylic acids, sulfonates, and emulsifiers. FA-series collectors consist of C8–C20 alkyl carboxylic acid and emulsifier.

The flotation effects of different composite collectors on RE minerals were investigated in the same conditions as those in the single reagent selection test. The results are shown in Figure 7.

Figure 7a shows that FHP composite collector exhibited poor collection abilities and selectivity, while the collection ability of L series collectors is relatively strong, especially L4 (same as the collector BK421B used by Zhang [42]) with good selectivity. Figure 7b shows that NQL and FA series collectors exhibited similar collection performances. In particular, FA301 and NQL exhibited the best collection ability, and the selectivity of FA301 was higher than that of the single collector OPS. When the REO grade was approximately 23%, the recovery was approximately 55%.

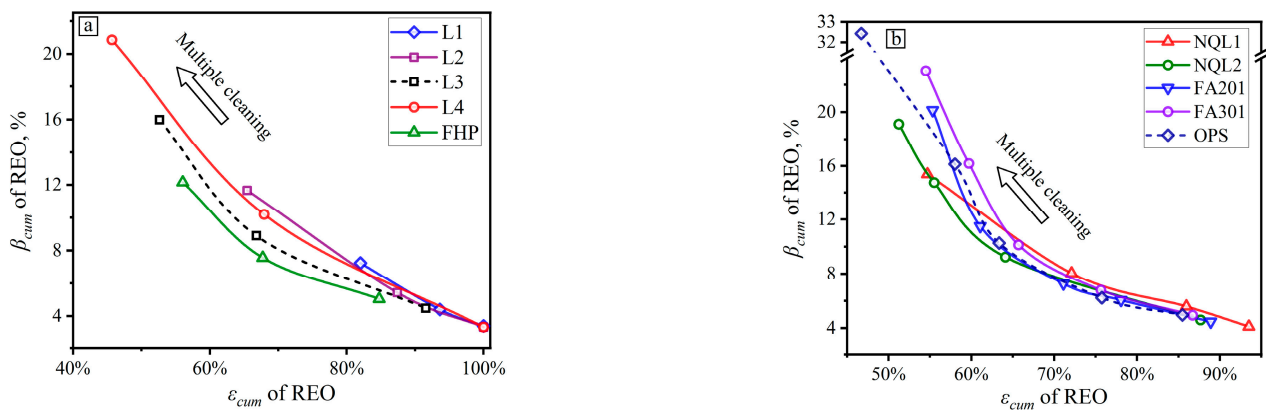


Figure 7. Relationship between the cumulative REO grade and recovery of flotation concentrates for different composite collectors. (a) L and FHP series collectors; (b) NQ, FA series collectors and OPS collector.

Overall, considering the REO grade and recovery of concentrate, FA301 was determined as the optimal collector for the flotation of RE ore and used in subsequent tests.

3.3. Determination of Flotation Conditions

3.3.1. Slurry Temperature and Collector Dosage

The slurry temperature and collector dosage were typically coupled. Increases in the slurry temperature and collector dosage may promote the floatability of Fe-containing minerals and lead to disordered floating. Therefore, the influences of pulp temperature and collector dosage on the flotation effect were investigated.

Figure 8 shows that at a given temperature, as the amount of collector increased, the cumulative REO recovery in the concentrate increased, and REO grade gradually decreased. In other words, the possibility of RE minerals floating increased at lower collector contents. With the increase in the collector consumption, increasing amounts of RE minerals were collected and enriched in the concentrate products. Moreover, as the excess collector combined with gangue minerals, more gangue minerals began to float and enter the concentrate, and disordered floating intensified. When the collector dosage increased to 400 g/t, the rate of increase in the cumulative REO recovery in the concentrate decreased. Therefore, the value of 400 g/t was considered appropriate for the roughing stage.

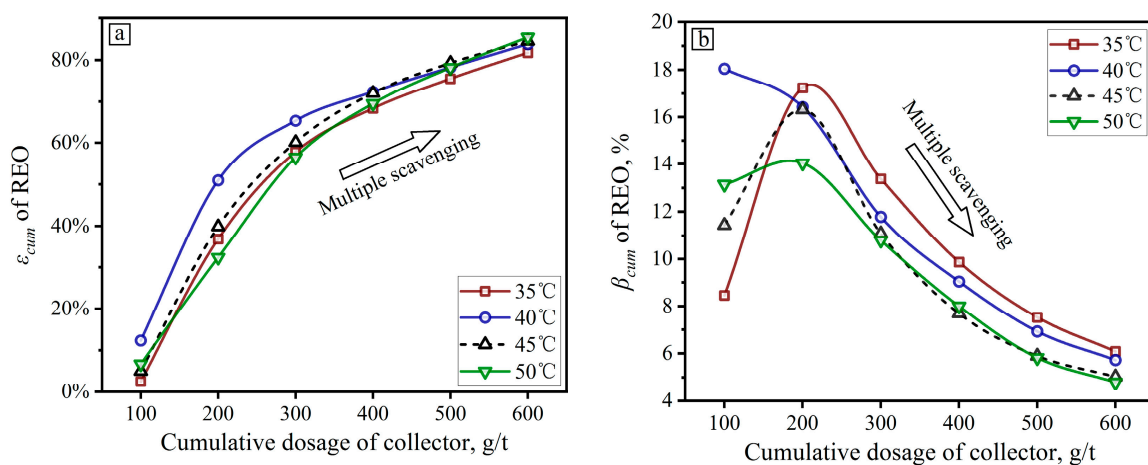


Figure 8. Relationships between collector dosages and ϵ_{cum} of REO (a), β_{cum} of REO (b) at different temperatures.

In particular, when the amount of the collector was 400 g/t, the concentrate yield gradually increased with the increase in the pulp temperature. In other words, as the temperature increased, the activity of gangue minerals was enhanced. The RE minerals and gangue minerals floated together, resulting in decreased REO grade in the concentrate (Figure 8b). The concentrate grade was reasonably high when the temperature was 35–40 °C. The rate of increase in the REO recovery was the highest when the slurry temperature was 40 °C, and the REO grade in the concentrate was close to the result of 35 °C and better than those at the other temperatures.

Therefore, the optimal slurry temperature was 40 °C and roughing collector dosage was 400 g/t, as in these conditions, the gangue materials did not considerably interact with the collector, and the floating of RE minerals was not adversely affected.

3.3.2. Inhibitor Dosage

Due to the high content of silicates in ore, the depression of silicate gangue minerals is important for RE minerals flotation. Figure 9a shows the variation in the REO recovery and grade of the flotation concentrate at different dosages of WG.

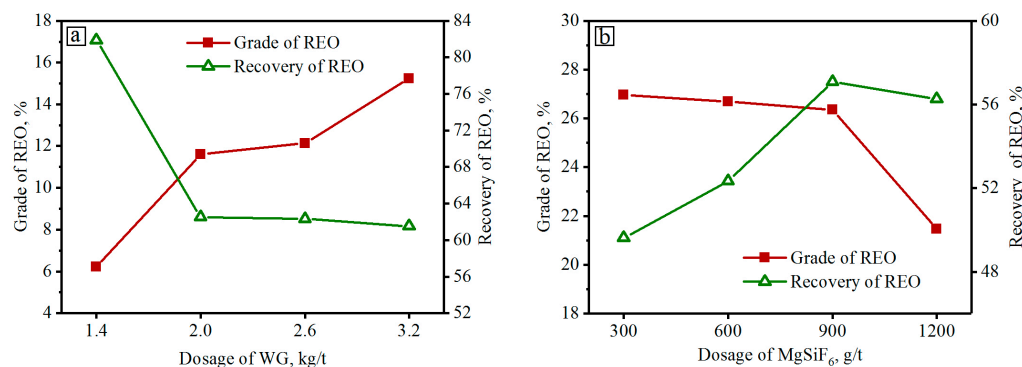


Figure 9. REO recovery and grade of the flotation concentrate at different dosages of WG (a) and MgSiF₆ (b).

As the WG dosage increased during roughing, the REO grade in the concentrate gradually increased and REO recovery gradually decreased. To recover the RE concentrate while maintaining a satisfactory REO grade, the WG dosage was set at 2 kg/t.

3.3.3. Activator Dosage

Fluorosilicates inhibit silicate gangue minerals and activate RE minerals [10]. Figure 9b shows the relationship between the REO recovery and grade of the flotation concentrate at different activator dosages. As the amount of MgSiF₆ increased, the REO recovery first increased and then decreased, whereas the concentrate grade gradually decreased. These trends indicated that gangue minerals were activated as the activator content increased. Therefore, the dosage of MgSiF₆ was set at 900 g/t.

3.3.4. Grinding Size

The previous mineralogy analysis results showed that RE minerals were closely associated with gangue minerals, so it is important to choose the appropriate grinding size to achieve liberation. Figure 10 shows the relationship between the REO grade and cumulative recovery of the flotation concentrate at different grinding sizes.

As the grinding time and amount of fine-grained components increased, the REO grade and recovery decreased. For the same concentrate grade, the REO recovery of the concentrate was the highest at the particle size of 50% < 38 μm, attributable to the increase in the dissociation degree as the ore particles became finer. Moreover, the disordered floating caused by ore slime worsened the flotation effect. Therefore, the particle size of the ore is determined to be 50% < 38 μm, for which the RE concentrate yield was 6.29%, REO grade was 32.013%, and recovery was 59.02%.

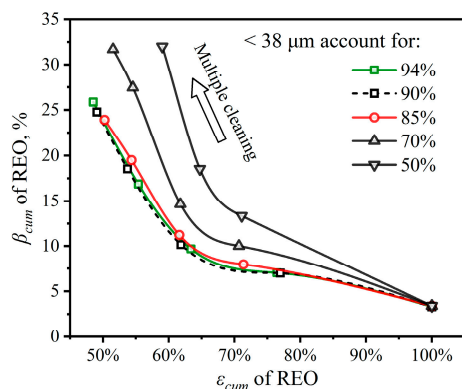


Figure 10. Relationship between the REO grade and cumulative recovery of the flotation concentrate at different grinding sizes.

3.4. Interaction between the Composite Collector and RE Minerals

The composite collector FA301 contains fatty acids, halogenated hydrocarbons, alcohols, and non-ionic surfactants with different carbon chain lengths. To clarify the underlying flotation mechanism, the flotation of RE minerals was characterised by zeta potential, FTIR, and XPS analyses.

3.4.1. Surface Potential of RE Minerals before and after Composite Collector Action

Zeta potentials were evaluated as a function of pH for each RE mineral (hingganite, monazite, and bastnaesite) treated with KCl solution (1 mM) in the absence and presence of FA301. The results are shown in Figure 11.

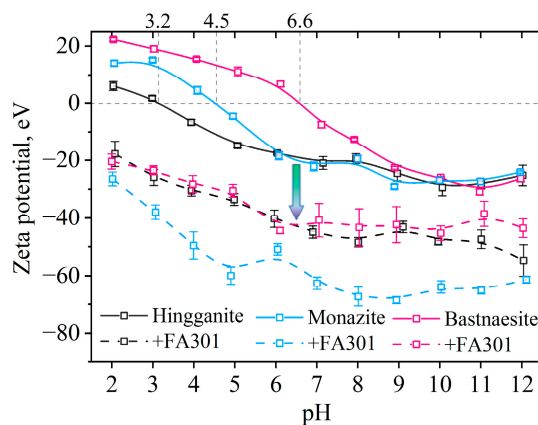


Figure 11. Relationship between the pH and zeta potential of RE minerals.

Zeta potential is the electrochemical potential of the interfacial double layer at the location of the shear plane relative to a point in the bulk solution away from the interface [20]. The change of zeta potential can reflect the adsorption of reagents on mineral surface, thus revealing the adsorption mechanism of reagents.

The pH value where the zeta potential is zero, the isoelectric point (IEP), is an important mineral property that can be used to characterise charging of the mineral surface [46]. As shown in Figure 11, the pure hingganite, monazite, and bastnaesite particles without FA301 exhibited IEPs at pH~3.2, ~4.5, and ~6.6, respectively. The surface of three RE minerals were hydroxylated and the surface zeta potential is negative at pH 8.6 (>IEP). Except for hingganite of which the zeta potential has not been reported before, the IEPs of monazite and bastnaesite were within the statistical range of Marion et al. [10] (Figure 12). The IEP of bastnaesite in this study showed a medium value in the range of the existing reported data. The IEP of monazite in this study was slightly lower than that reported

by others, which may be related to the differences in the origin or chemical composition of monazite.

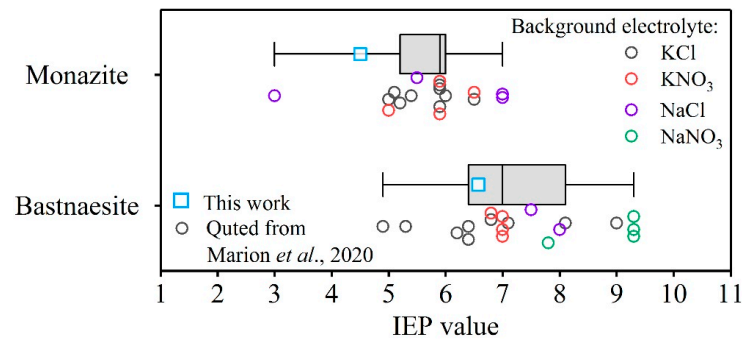


Figure 12. The IEPs of monazite and bastnaesite measured in this work and reported previously [10].

After conditioned with FA301, zeta potential of each RE mineral throughout the pH range shifted negatively and the IEP was reduced to pH < 2. The negative shift of zeta potential of monazite observed in the presence of FA301 was the most obvious, followed by bastnaesite, and the smallest in hingganite, which may be related to the difference in the density of surface active sites. The negative shift of zeta potential indicated that anions were the active components of FA301, which had overcome the electrostatic repulsion and chemically adsorbed on the surface of RE minerals. The addition of FA301 to bastnaesite in KCl solution led to a sharp decrease in the zeta potential with decreasing pH especially below its IEP, suggesting that some anions in the collector had also adsorbed on the surface of bastnaesite by electrostatic adsorption.

3.4.2. Substance Structure of Mineral Surface after Composite Collector Adsorption

FTIR analyses were performed to clarify the substance structure of the collector on the mineral surface. Specifically, the infrared spectral characteristics of the collector adsorbed onto hingganite, monazite, and bastnaesite were investigated, as shown in Figure 13.

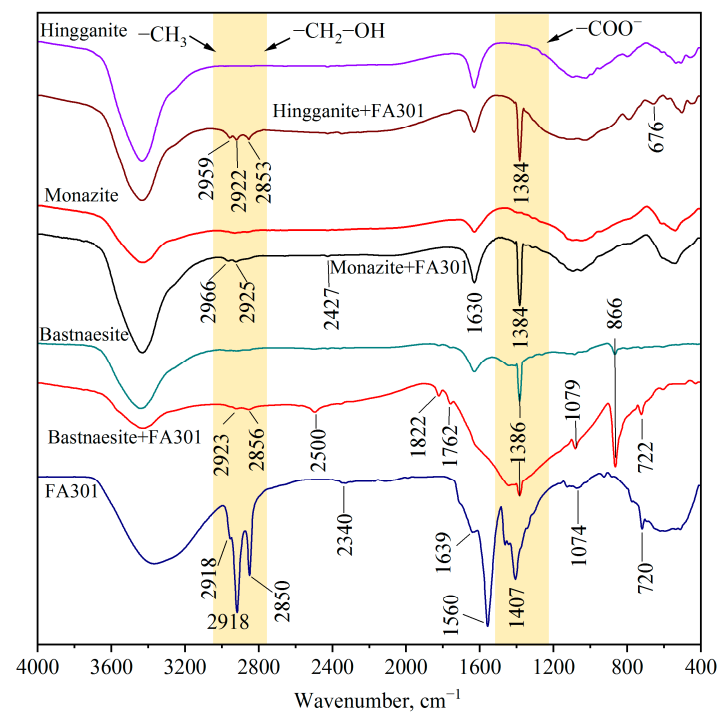


Figure 13. Infrared spectral characteristics of the collector before and after its interaction with hingganite, monazite, and bastnaesite.

As shown in Figure 13, stretching vibration absorption peaks of $-\text{CH}_3$ and $-\text{CH}_2$ -hydrocarbon groups were observed at 2850, 2918, and 2955 cm^{-1} [47], and symmetric stretching vibration peaks of $-\text{COO}^-$ were observed at 1407 and 1560 cm^{-1} . The vibration contraction peak of the hydroxyl group in the crystal structure was located at 3500–3580 cm^{-1} . After the interaction with FA301, the stretching vibration absorption peaks of $-\text{CH}_3$ and $-\text{CH}_2\text{-OH}$ at 2853, 2922, and 2959 cm^{-1} intensified on the surface of hingganite. Compared with the absorption peaks at 2849, 2918, and 2955 cm^{-1} , different degrees of deviation were observed, indicating stable adsorption of the collector on the mineral surface. The symmetrical stretching vibration peak of $-\text{COO}^-$ at 1384 cm^{-1} appeared at the surface of hingganite after flotation, with a deviation larger than that of the peak of 1407 cm^{-1} in FA301. This larger deviation likely occurred because the carboxyl functional group directly adsorbed onto the mineral surface, and the chemical bond morphology was altered. This increase indicated that the collector chemically adsorbed onto the mineral surface during the flotation process, and the active component was carboxylic acid molecules.

In the infrared spectrum of monazite (Figure 13), peaks at 618 and 1051 cm^{-1} were observed, corresponding to the stretching vibration absorption peaks of PO_4^{3-} [48]. After the interaction with FA301, several new spectral peaks appeared on the monazite surface, with 1384 cm^{-1} corresponding to the symmetric stretching vibration peak of $-\text{COO}^-$ and 2925 and 2966 cm^{-1} corresponding to the stretching vibration absorption peaks of $-\text{CH}_3$ and $-\text{CH}_2\text{-OH}$, respectively. The peak positions of collectors at 1407, 2850, and 2955 cm^{-1} were offset, indicating that the collector chemically adsorbed onto the monazite surface.

The peaks at 866 and 1386 cm^{-1} in the infrared spectrum of bastnaesite (Figure 13) corresponded to the out-of-plane bending and stretching vibration absorption peaks of CO_3^{2-} in the mineral lattice, respectively. Several new spectral peaks appeared on the surface of bastnaesite after its interaction with the collector, including the C–H stretching vibration peak at 2856 and 2923 cm^{-1} , the $-\text{COO}^-$ stretching vibration peak at 722 cm^{-1} , and the C–O absorption peak of adipose ethers or esters at 1079 cm^{-1} . The wide carboxylic acid ($-\text{COO}^-$) absorption peak between 1200 and 1560 cm^{-1} was superimposed with the original CO_3^{2-} absorption peak at 1386 cm^{-1} . The carboxylic acid group was expected to be the main functional group contributing to the collection effect. All of the new absorption peaks deviated from the peaks in the collector to different degrees, indicating the generation of new bond cooperation. This observation was consistent with the conclusion that the collector chemically adsorbed onto the mineral surface. The presence of C–O absorption peaks indicated not only the adsorption of fatty acids but also the presence of ethers or esters.

3.4.3. Adsorption Sites of the Composite Collector on the Surface of RE Minerals

The adsorption sites of the collector on the surface of RE minerals were examined to promote the development of novel efficient collectors. Specifically, XPS analysis was performed to examine the changes in the surface element composition and valence states of hingganite, monazite, and bastnaesite before and after their treatment with the collector. Moreover, the narrow spectrum scanning of the binding energy of the main elements on the mineral surface before and after flotation was performed. The fitting results of hingganite are shown in Figure 14. The fitting results of monazite and bastnaesite are shown in Figures S2 and S3.

Figure 14 shows the XPS results of hingganite ((Y, Ce, La)[BeSiO₄](OH)). The REEs Y, La, and Ce were noted to exist in the combined states of Y(III), La(III), and Ce(IV), respectively. Trace amounts of praseodymium (Pr) in the form of Pr(III) were indicated by a weak and fuzzy spectral peak. The characteristic element Be of hingganite existed in the valence state of Be(II), and silicon (Si) existed in the Si–O form. The spectral peak at 848.6 eV on the mineral surface corresponded to Fe2s in the form of homomorphism. According to the comparison of the binding energy on the mineral surface before and after flotation, the Be and Si states on the surface of hingganite did not change significantly. In contrast, the

spectral peaks of Y, La, Ce, and Pr deviated to varying degrees from -0.4 to $+0.4$ eV. This deviation may be affected by the test error, but considering the IR spectral characteristics, it may indicate that after the interaction of hingganite with the collector, new chemical bonds formed on the mineral surface, and the main active sites of the collector were Y, La, Ce, and Pr.

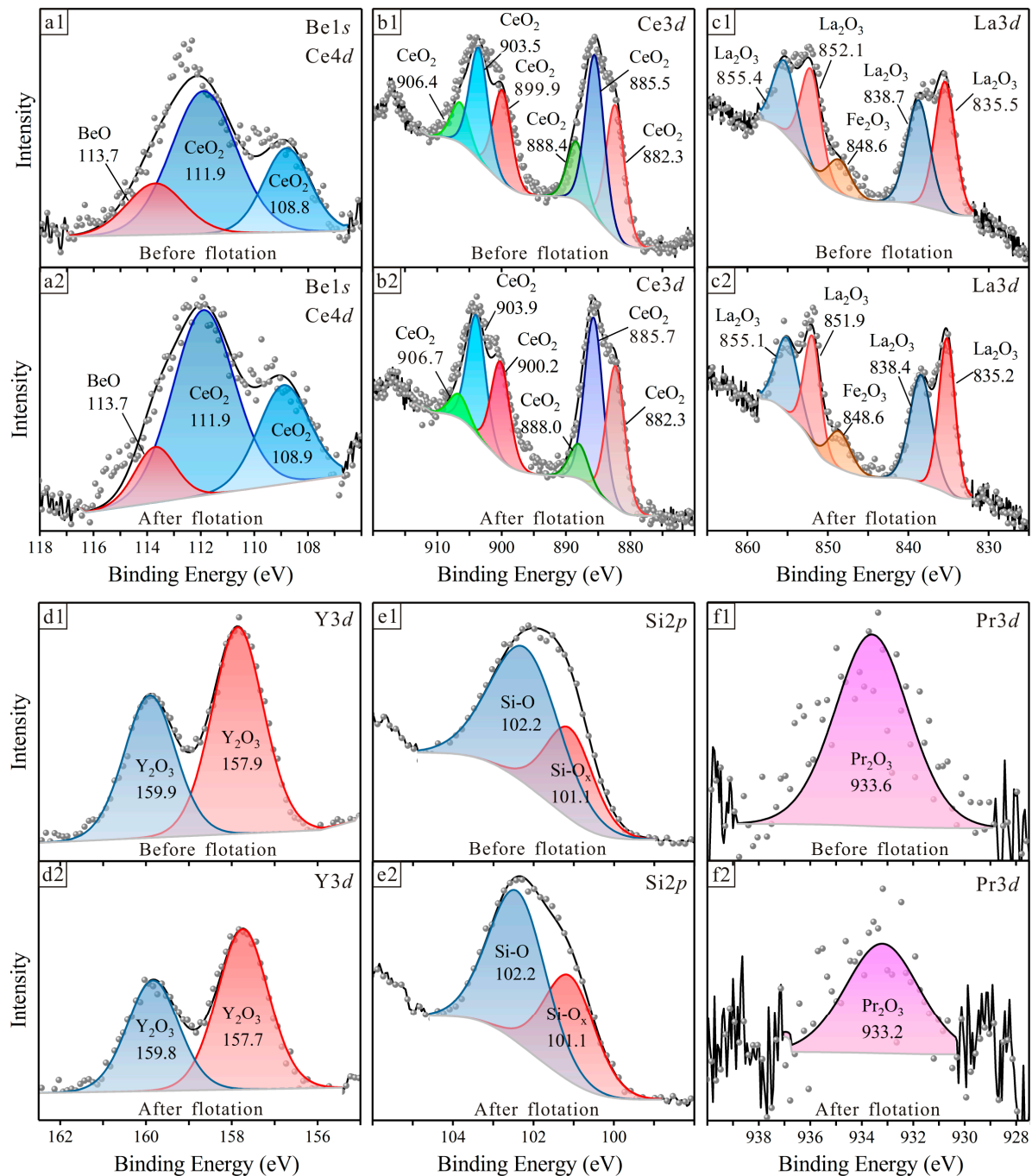


Figure 14. XPS characteristics of hingganite surface elements before and after flotation. (a) Be1s and Ce4d; (b) Ce3d; (c) La3d; (d) Y3d; (e) Si2p; (f) Pr3d.

Figure S2 shows the XPS results of monazite ($(\text{Ce}_{0.5}, \text{La}_{0.25}, \text{Nd}_{0.2}, \text{Th}_{0.05})(\text{PO}_4)$) before and after flotation. According to the spectral peak fitting results, La and Ce on the monazite surface mainly existed in the forms of La(III) and Ce(III) and Ce(IV), respectively. P and Th existed in the combined states of REPO_4 and ThO_2 , respectively. After the interaction with

the collector, the binding energies of La, Ce, P, and Th deviated to varying degrees. La and Ce may be the main sites of collector action on the surface of monazite.

Figure S3 shows the XPS results of bastnaesite $((La_{0.6}, Ce_{0.4})(CO_3)F)$ before and after its interaction with the collector. According to the spectral peak fitting results, La, Ce, and Nd on the mineral surface existed in the forms of La(III), Ce(IV), and Nd(III), respectively. In addition to the contaminant form (248.8 eV), carbon (C) was present in the form of MCO_3 metal compounds. After the interaction with the collector, the binding energies of La, Ce, and Nd deviated from the range of -1.2 eV to $+0.5$ eV, with the most significant deviation pertaining to La. La may be the main active site for the adsorption of the collector onto the surface of bastnaesite, consistent with the results for hingganite and monazite.

4. Conclusions

An efficient composite collector was developed for alkaline rock RE ores containing various RE minerals and Fe-containing minerals. The flotation performances of 25 collectors (including carboxylic acids (salts), hydroxamic acids, organic phosphoric acids, and sulfonates) were compared. The results indicated that the flotation effect of RE minerals was not satisfactory when only a single collector was used. The composite collector FA301 with different carbon chain lengths was identified as the optimal collector.

Other conditions were also optimised. The optimal configuration for the flotation of alkaline rock-type RE involved one stage of roughing, one stage of scavenging, and two stages of cleaning. The particle size of $50\% < 38 \mu m$, dosages of the regulator (Na_2CO_3), collector (FA301), WG, magnesium fluosilicate, and FA301 (scavenging) were 1 kg/t, 400 g/t, 2 kg/t, 900 g/t, and 200 g/t, respectively, and the pulp temperature was $40^\circ C$.

By adjusting the pulp temperature and type and dosage of the preferred collector, a variety of RE minerals were recovered efficiently, and the introduction of other gangue minerals could be prevented. RE concentrates with a yield of 6.29%, REO grade of 32.013%, and recovery of 59.02% were achieved by flotation.

The composite collector FA301 chemically adsorbed onto the surface of hingganite, monazite, and bastnaesite, with the carboxyl group serving as the main functional group contributing to the collection effect.

The REEs La, Ce, and Y should be the main active sites on the surface of RE minerals, and the collector FA301 induced the collection effect by forming new chemical bonds with these REEs on the surface of minerals, as shown in Figure 15. Overall, to develop efficient RE mineral collectors, reagents with carboxylic acid structures that can easily combine with La, Ce, Y, and other REEs and exhibit different carbon chain lengths must be further explored.

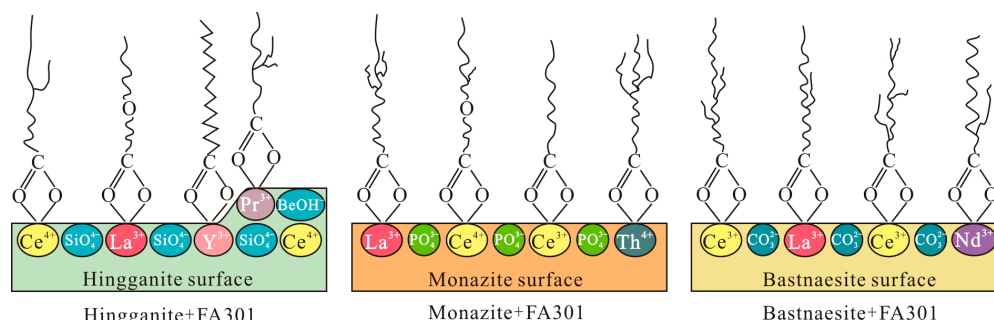


Figure 15. Schematic representation of adsorption mechanism of composite collector FA301 on the surface of RE minerals.

Supplementary Materials: The following supporting information can be downloaded at: <https://www.mdpi.com/article/10.3390/min13081025/s1>, Figure S1: SEM images and energy spectra of RE minerals; Figure S2: Comparison of XPS characteristics of monazite before and after flotation; Figure S3: Comparison of XPS characteristics of bastnaesite before and after flotation;

Table S1: Reagents used in the flotation tests; Table S2: The specific descriptions of flotation condition tests; Table S3: Mineralogical composition of the as-prepared HIMS concentrates.

Author Contributions: Conceptualization, Z.L. (Zhichao Liu), Z.L. (Zhenjiang Liu) and C.L.; investigation, C.L. and Z.L. (Zhenjiang Liu); supervision, Z.L. (Zhichao Liu) and J.L.; writing—original draft, C.L.; writing—review and editing, Z.L. (Zhichao Liu), G.L., Y.T. and M.Z. All authors have read and agreed to the published version of the manuscript.

Funding: This research was funded by the Joint Fund (Key program U2067201) for Nuclear Technology Innovation Sponsored by the National Natural Science Foundation of China and the China National Nuclear Corporation, the China National Nuclear Corporation (CNNC) Science Fund for Talented Young Scholars (No. CNNC-2020-13), and the Nuclear Energy Development Scientific Research Project.

Data Availability Statement: Data is contained within the article or supplementary material.

Conflicts of Interest: The authors declare no conflict of interest.

References

1. Chakhmouradian, A.R.; Wall, F. Rare earth elements: Minerals, mines, magnets (and more). *Elements* **2012**, *8*, 333–340. [[CrossRef](#)]
2. Hatch, G.P. Dynamics in the global market for rare earths. *Elements* **2012**, *8*, 341–346. [[CrossRef](#)]
3. Nassar, N.T.; Du, X.; Graedel, T.E. Criticality of the rare earth elements. *J. Ind. Ecol.* **2015**, *19*, 1044–1054. [[CrossRef](#)]
4. Dostal, J. Rare earth element deposits of alkaline igneous rocks. *Resources* **2017**, *6*, 34. [[CrossRef](#)]
5. Chakhmouradian, A.R.; Zaitsev, A.N. Rare earth mineralization in igneous rocks: Sources and processes. *Elements* **2012**, *8*, 347–353. [[CrossRef](#)]
6. Dostal, J. Rare metal deposits associated with alkaline/peralkaline igneous rocks. In *Rare Earth and Critical Elements in Ore Deposits*, 1st ed.; Verplanck, P.L., Hitzman, M.W., Eds.; Society of Economic Geologists Inc.: Littleton, CO, USA, 2016; Volume 2, pp. 33–54. [[CrossRef](#)]
7. Goodenough, K.M.; Wall, F.; Merriman, D. The rare earth elements: Demand, global resources, and challenges for resourcing future generations. *Nat. Resour. Res.* **2017**, *27*, 201–216. [[CrossRef](#)]
8. Jordens, A.; Cheng, Y.; Waters, K.E. A review of the beneficiation of rare earth element bearing minerals. *Miner. Eng.* **2013**, *41*, 97–114. [[CrossRef](#)]
9. Yang, X.; Satur, J.V.; Sanematsu, K.; Laukkanen, J.; Saastamoinen, T. Beneficiation studies of a complex REE ore. *Miner. Eng.* **2015**, *71*, 55–64. [[CrossRef](#)]
10. Marion, C.; Li, R.; Waters, K.E. A review of reagents applied to rare-earth mineral flotation. *Adv. Colloid Interface Sci.* **2020**, *279*, 102142. [[CrossRef](#)]
11. Beard, C.D.; Goodenough, K.M.; Borst, A.M.; Wall, F.; Siegfried, P.R.; Dedy, E.A.; Pohl, C.; Hutchison, W.; Finch, A.A.; Walter, B.F.; et al. Alkaline-silicate REE-HFSE systems. *Econ. Geol.* **2023**, *118*, 177–208. [[CrossRef](#)]
12. Vasyukova, O.V.; Williams-Jones, A.E. Direct measurement of metal concentrations in fluid inclusions, a tale of hydrothermal alteration and REE ore formation from Strange Lake, Canada. *Chem. Geol.* **2018**, *483*, 385–396. [[CrossRef](#)]
13. Wu, M.; Samson, I.M.; Qiu, K.; Zhang, D. Concentration mechanisms of rare earth element-Nb-Zr-Be mineralization in the Baerzhe deposit, Northeast China: Insights from textural and chemical features of amphibole and rare metal minerals. *Econ. Geol.* **2021**, *116*, 651–679. [[CrossRef](#)]
14. Filippov, L.O.; Dehaine, Q.; Filippova, I.V. Rare earths (La, Ce, Nd) and rare metals (Sn, Nb, W) as by-products of kaolin production—Part 3: Processing of fines using gravity and flotation. *Miner. Eng.* **2016**, *95*, 96–106. [[CrossRef](#)]
15. Abaka-Wood, G.B.; Addai-Mensah, J.; Skinner, W. A study of flotation characteristics of monazite, hematite, and quartz using anionic collectors. *Int. J. Miner. Process.* **2017**, *158*, 55–62. [[CrossRef](#)]
16. Zhang, J.; Zhao, B.; Schreiner, B. Rare earth beneficiation and hydrometallurgical processing. In *Separation Hydrometallurgy of Rare Earth Elements*, 1st ed.; Zhang, J., Zhao, B., Schreiner, B., Eds.; Springer Cham Inc.: Cham, Switzerland, 2016; Volume 2, pp. 19–54. [[CrossRef](#)]
17. Gong, W. Use of the QEM*SEM analysis in flotation testwork on a phosphate ore containing monazite. *Int. J. Miner. Process.* **1993**, *37*, 89–108. [[CrossRef](#)]
18. Cao, S.; Cao, Y.; Liao, Y.; Ma, Z. Depression mechanism of strontium ions in bastnaesite flotation with salicylhydroxamic acid as collector. *Minerals* **2018**, *8*, 66. [[CrossRef](#)]
19. Jordens, A.; Marion, C.; Kuzmina, O.; Waters, K.E. Physicochemical aspects of allanite flotation. *J. Rare Earths* **2014**, *32*, 476–486. [[CrossRef](#)]
20. Jordens, A.; Marion, C.; Kuzmina, O.; Waters, K.E. Surface chemistry considerations in the flotation of bastnäsite. *Miner. Eng.* **2014**, *66–68*, 119–129. [[CrossRef](#)]
21. Sarvaramini, A.; Azizi, D.; Larachi, F. Hydroxamic acid interactions with solvated cerium hydroxides in the flotation of monazite and bastnäsite—Experiments and DFT study. *Appl. Surf. Sci.* **2016**, *387*, 986–995. [[CrossRef](#)]

22. Yang, Z.; Wu, W.; Bian, X. Synthesis of 3-hydroxy-2-naphthyl hydroxamic acid collector: Flotation performance and adsorption mechanism on bastnaesite. *J. South. Afr. Inst. Min. Metall.* **2017**, *117*, 593–598. [CrossRef]
23. Sastri, V.S.; Bünzli, J.C.; Rao, V.R.; Rayudu, G.V.S.; Perumareddi, J.R. Stability of complexes. In *Modern Aspects of Rare Earths and Their Complexes*, 1st ed.; Sastri, V.S., Bünzli, J., Rao, V.R., Rayudu, G.V.S., Perumareddi, J.R., Eds.; Elsevier: Amsterdam, The Netherlands, 2003; Volume 3, pp. 127–257. [CrossRef]
24. Khalil, M.M.; Fazary, A.E. Potentiometric studies on binary and ternary complexes of di- and trivalent metal ions involving some hydroxamic acids, amino acids, and nucleic acid components. *Mon. Chem.* **2004**, *135*, 1455–1474. [CrossRef]
25. Stark, T.; Silin, I.; Wotruba, H. Mineral processing of eudialyte ore from Norra Kärr. *J. Sust. Metall.* **2017**, *3*, 32–38. [CrossRef]
26. Bulatovic, S.M. Flotation of REO minerals. In *Handbook of Flotation Reagents: Chemistry, Theory and Practice*, 1st ed.; Bulatovic, S.M., Ed.; Elsevier: Amsterdam, The Netherlands, 2010; Volume 2, pp. 151–173. [CrossRef]
27. Chi, R.; Wang, D. *Mineral Processing of Rare Earth Minerals*, 1st ed.; Science Press: Beijing, China, 2014; pp. 119–265.
28. Li, R.; Marion, C.; Espiritu, E.R.L.; Multani, R.; Sun, X.; Waters, K.E. Investigating the use of an ionic liquid for rare earth mineral flotation. *J. Rare Earths* **2021**, *39*, 866–874. [CrossRef]
29. Kursun, I.; Terzi, M.; Ozdemir, O. Determination of surface chemistry and flotation properties of rare earth mineral allanite. *Miner. Eng.* **2019**, *132*, 113–120. [CrossRef]
30. Fawzy, M.M. Surface characterization and froth flotation of fergusonite from Abu Dob pegmatite using a combination of anionic and nonionic collectors. *Physicochem. Probl. Mineral. Pro.* **2018**, *54*, 677–687. [CrossRef]
31. Natarajan, R. Hydroxamic acids as chelating mineral collectors. In *Hydroxamic Acids*, 1st ed.; Gupta, S.P., Ed.; Springer: Berlin/Heidelberg, Germany, 2013; Volume 11, pp. 281–307. [CrossRef]
32. Liu, W.; Wang, X.; Wang, Z.; Miller, J.D. Flotation chemistry features in bastnaesite flotation with potassium lauryl phosphate. *Miner. Eng.* **2016**, *85*, 17–22. [CrossRef]
33. Sun, L.; Hu, Y.; Sun, W. Effect and mechanism of octanol in cassiterite flotation using benzohydroxamic acid as collector. *Trans. Nonferrous Met. Soc. China* **2016**, *26*, 3253–3257. [CrossRef]
34. Filippova, I.V.; Filippov, L.O.; Duverger, A.; Severov, V.V. Synergetic effect of a mixture of anionic and nonionic reagents: Ca mineral contrast separation by flotation at neutral pH. *Miner. Eng.* **2014**, *66–68*, 135–144. [CrossRef]
35. Xu, L.; Tian, J.; Wu, H.; Lu, Z.; Sun, W.; Hu, Y. The flotation and adsorption of mixed collectors on oxide and silicate minerals. *Adv. Colloid Interface Sci.* **2017**, *250*, 1–14. [CrossRef]
36. Yang, S.; Xu, Y.; Liu, C.; Soraya, D.A.D.; Li, C.; Li, H. Investigations on the synergistic effect of combined NaOl/SPA collector in ilmenite flotation. *Colloid Surf. A Physicochem. Eng. Asp.* **2021**, *628*, 127267. [CrossRef]
37. Xu, Y.; Xu, L.; Wu, H.; Wang, Z.; Shu, K.; Fang, S.; Zhang, Z. Flotation and co-adsorption of mixed collectors octanohydroxamic acid/sodium oleate on bastnaesite. *J. Alloys Compd.* **2020**, *819*, 152948. [CrossRef]
38. Bao, X.; Xing, Y.; Liu, Q.; Liu, J.; Dai, S.; Gui, X.; Li, J.; Yang, Z. Investigation on mechanism of the oleic acid/methyl oleate/diesel ternary compound collector in low-rank coal flotation. *Fuel* **2022**, *320*, 123894. [CrossRef]
39. Luo, L.; Wu, H.; Xu, L.; Meng, J.; Lu, J.; Zhou, H.; Huo, X.; Huang, L. An in situ ATR-FTIR study of mixed collectors BHA/DDA adsorption in ilmenite-titanaugite flotation system. *Int. J. Min. Sci. Technol.* **2021**, *31*, 689–697. [CrossRef]
40. Qiao, X.; Liu, A.; Li, Z.; Fan, J.; Luo, C.; Fan, P.; Liu, Y.; Fan, M. A novel miscible collector DDA–2-octanol–kerosene: Properties and flotation performance. *Miner. Eng.* **2020**, *156*, 106475. [CrossRef]
41. Yang, W.; Niu, H.; Li, N.; Hollings, P.; Zurevinski, S.; Xing, C. Enrichment of REE and HFSE during the magmatic-hydrothermal evolution of the Baerzhe alkaline granite, NE China: Implications for rare metal mineralization. *Lithos* **2020**, *358–359*, 105411. [CrossRef]
42. Zhang, Y. *Experimental Study on 801 Ore Dressing Technology in Zhalute Banner, Inner Mongolia*; Beijing General Research Institute of Mining and Metallurgy: Beijing, China, 2017.
43. Su, H.; Jiang, S.; Zhu, X.; Duan, Z.; Huang, X.; Zou, T. Magmatic-hydrothermal processes and controls on rare-metal enrichment of the Baerzhe peralkaline granitic pluton, inner Mongolia, northeastern China. *Ore. Geol. Rev.* **2021**, *131*, 103984. [CrossRef]
44. Zhang, X.; Li, C.; Liu, Z.; Li, L.; Zhou, M.; Ma, Y. Pre-concentration of complicated rare-earth mineral bearing ore by wet electromagnetic separation and superconducting magnetic separation. *At. Energy. Sci. Technol.* **2022**, *56*, 225–234.
45. Naumkin, A.V.; Kraut-Vass, A.; Gaarenstroom, S.W.; Powell, C.J. NIST X-ray Photoelectron Spectroscopy Database. Available online: <https://srdata.nist.gov/xps/Default.aspx> (accessed on 8 March 2022).
46. Pope, M.I.; Sutton, D.I. The correlation between froth flotation response and collector adsorption from aqueous solution. Part I. Titanium dioxide and ferric oxide conditioned in oleate solutions. *Powder Technol.* **1973**, *7*, 271–279. [CrossRef]
47. Workman, J.J.; Weyer, L. *Practical Guide to Interpretive Near-Infrared Spectroscopy*, 1st ed.; CRC Press Inc.: Boca Raton, FL, USA, 2007; pp. 23–62. [CrossRef]
48. Azizi, D.; Larachi, F.; Latifi, M. Ionic-liquid collectors for rare-earth minerals flotation—Case of tetrabutylammonium bis(2-ethylhexyl)-phosphate for monazite and bastnaesite recovery. *Colloid Surf. A Physicochem. Eng. Asp.* **2016**, *506*, 74–86. [CrossRef]

Disclaimer/Publisher’s Note: The statements, opinions and data contained in all publications are solely those of the individual author(s) and contributor(s) and not of MDPI and/or the editor(s). MDPI and/or the editor(s) disclaim responsibility for any injury to people or property resulting from any ideas, methods, instructions or products referred to in the content.